**ISSN**: 1231-4005
**e-ISSN:** 2354-0133
**DOI:** 10.5604/01.3001.0010.2817

# INFLUENCE OF THE ATMOSPHERIC TURBULENCE ON THE ACCURACY OF THE MISSILE TARGETING

**Grzegorz Kowaleczko**

*Polish Air Force Academy*
*Dywizjonu 303 Street 35, 08-521 Deblin, Poland*
*tel.: +48 815517423, fax: +48 815517417, e-mail: g.kowaleczko@chello.pl*

**Romuald Kaźmierczak**

*Air Force Institute of Technology*
*Ksiecia Boleslawa Street 6, 01-494 Warsaw, Poland*
*tel.: +48 261 85 13 02, fax: +48 261 85 13 13, e-mail: Romuald.kazmierczak@itwl.pl*

***Abstract***

*The article presents results of simulation of 6-DOF motion for a missile subjected to atmospheric turbulences. Therefore, an applied mathematical model of motion includes description of stochastic turbulences influencing on missile flight. Both models of the motion as well as of turbulences are shortly presented. Model validity was assessed by comparing the calculation results with the data recorded during shooting on the range. Result of series of simulations allows determining the missile sensitivity to this case of disturbances. Exemplary results of simulations are shown.*

*The turbulence model assumes that the wind is dependent on time and space. This assumption is based on the Taylor's "frozen turbulence" hypothesis. The advection velocity of the turbulence is much greater than the velocity scale of the turbulence itself. The velocity has two component. In the article, the first component is omitted and the second is treated as the stochastic process representing atmospheric turbulence. To describe this turbulence Shinozuka's method was applied. Mathematical description of the missile motion, equations of translatory motion, External forces end moments, model of the turbulence are presented in the article.*

***Keywords:*** *missile dynamics, stochastic turbulences, numerical simulations*

## 1. Introduction

A maximum accuracy and precision are the main goal during missile shooting, which can be performed in various atmospheric conditions. Aerodynamic forces are the main forces acting on the missiles. They directly depend on the missile velocity relative to the air. Therefore, atmospheric turbulences may be a significant factor affecting the missile motion. Depending on them a different point on the Earth's surface can be reached. This means that turbulences influence on the accuracy and precision of the missile. The main problem is to determine the sensitivity of the missile to this kind of disturbances. This problem can be resolved experimentally or in the way of theoretical investigations.

To resolve this problem theoretically the 6-DOF mathematical model of missile motion has to be applied. We can find a lot of similar each other models in the literature [1-4, 6, 12, 15-17, 20]. In this article, a model of the missile with variable mass is used. It is described in details in [8]. This model includes changes of missile mass characteristics during burning process. Thrust is not treated as the external force and is calculated on the basis of a solution of inner ballistic problems [8, 10, 11, 23, 24]. The used model also describes the jet damping effect [21], but this effect is the second of importance, as it is shown in [8].

Applied in this article description of atmospheric turbulences takes into account stochastic character of the wind field. To determine this field, the Shinozuka's method was applied. It was originally used to model earthquakes [18, 19]; and is adopted to simulate turbulences treated as the stochastic processe [9, 13].

## 2. Mathematical description of the missile motion

*Coordinate systems*

The following orthogonal coordinate systems were used to determine motion equations of the missile: $Ox_g y_g z_g$ – the Earth-referenced system with its origin $O$ at any fixed point of the missile, $Oxyz$ – the missile-fixed system with the origin at point $O$, $Ox_a y_a z_a$ – the air trajectory reference frame. The origin $O$ is the centre of mass of the missile after the combustion process.

These systems are related to each other by means of the following angles: ($\Psi$ – yaw, $\Theta$ – pitch, $\Phi$ – roll) for systems $O_g x_g y_g z_g$ and $Oxyz$ and ($\alpha$ – angle of attack, $\beta$ – sideslip angle) for systems $O_g x_g y_g z_g$ and $Oxyz$. The transformation matrices between systems /from $Ox_g y_g z_g$ to $Oxyz$ and from $Ox_a y_a z_a$ to $Oxyz$/ are as follows:

$$\mathbf{L}_{m/g} = \begin{bmatrix} cP \cdot cT & sP \cdot cT & -sT \\ cP \cdot sT \cdot sF - sP \cdot cF & sP \cdot sT \cdot sF + cP \cdot cF & cT \cdot sF \\ cP \cdot sT \cdot cF + sP \cdot sF & sP \cdot sT \cdot cF - cP \cdot sF & cT \cdot cF \end{bmatrix}, \quad \mathbf{L}_{m/a} = \begin{bmatrix} cA \cdot cB & -cA \cdot sB & -sA \\ sB & cB & 0 \\ sA \cdot cB & -sA \cdot sB & cA \end{bmatrix}, \tag{1}$$

where: $cP=\cos\Psi$, $sP=\sin\Psi$, $cT=\cos\Theta$, $sT=\sin\Theta$, $cF=\cos\Phi$, $sF=\sin\Phi$, $cA=\cos\alpha$, $sA=\sin\alpha$, $cB=\cos\beta$, $sB=\sin\beta$.

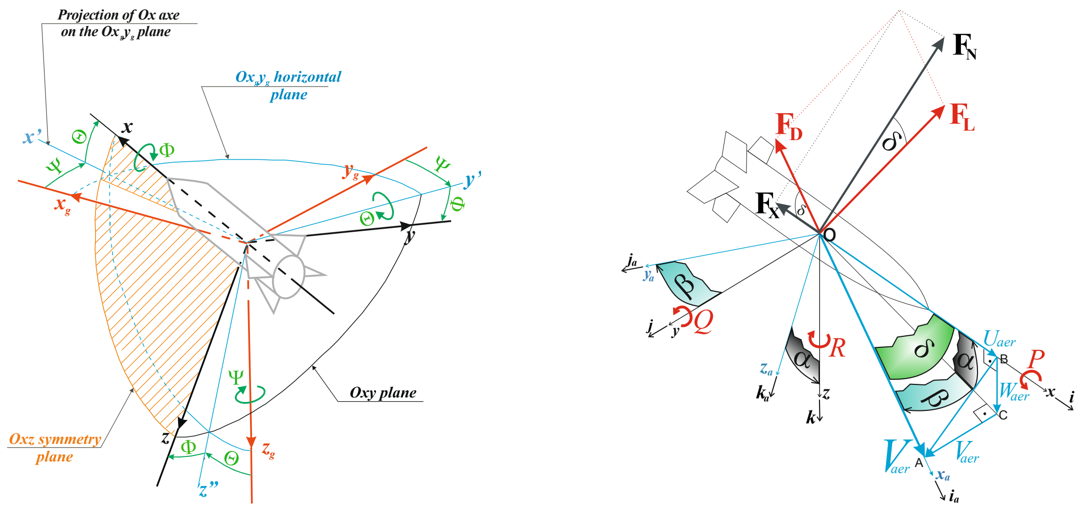


*Fig. 1. Coordinate systems, static aerodynamic forces, angles and velocities*

## 3. Equations of translatory motion

In *Oxyz,* system six scalar equations of translatory and rotational motions taken from [8] are as follows:

$$m(\dot{U} + QW - RV) - S_x(Q^2 + R^2) + ma_{x\_rel\_C} + \ddot{m}(x_C - x_E) + 2\dot{m}U_{rel\_C} = F_x + T, \tag{2a}$$

$$m(\dot{V} + RU - PW) + S_x(PQ + \dot{R}) + 2mRU_{rel\_C} + 2\dot{m}R(x_C - x_E) = F_y, \tag{2b}$$

$$m(\dot{W} + PV - QU) + S_x(PR - \dot{Q}) - 2mQU_{rel\_C} - 2\dot{m}Q(x_C - x_E) = F_z, \tag{2c}$$

$$I_x \dot{P} = L, \tag{2d}$$

$$I_y \dot{Q} + PR(I_x - I) - S_x(\dot{W} + PV - QU) + 2Q\sum_i m_i x_i U_{rel\_i} = M, \tag{2e}$$

$$I_z \dot{R} + PQ(I - I_x) + S_x(\dot{V} + RU - PW) + 2R\sum_i m_i x_i U_{rel\_i} = N, \tag{2f}$$

where we have: $m = m_{fuselage} + m_{fuel} + m_{chamber} + m_{nozzle}$ – missile mass, $\dot{m} = \dot{m}_{fuel}$ – mass flow rate, $\ddot{m} = \ddot{m}_{fuel}$ – acceleration of mass change, ($I_x$, $I_y$, $I_z$) – inertia moments, ($m_i$, $x_i$) – mass and coordinate of $i$-th elementary mass of the combustion products inside the missile, $\mathbf{V}_O = [U, V, W]^T$ – the velocity of the pole $O$ relative to the Earth, $\boldsymbol{\omega} = [P, Q, R]^T$ – the angular velocity of the missile, – $S_x = \sum_i x_i m_i$ – the static moment of the missile, $x_C = S_x / m$ – the coordinate of the mass centre, $x_E$ – the coordinate of the nozzle exit, $U_{rel\_C} = \dot{m} \cdot \frac{x_{fuel} - x_C}{m}$ – the relative velocity of the mass centre, $a_{x\_rel\_C} = -2\frac{\dot{m}}{m} U_{rel\_C}$ – the relative velocity of the mass centre, $\mathbf{F} = [F_x, F_y, F_z]^T$ – the sum of aerodynamic and gravitational forces, $T$ – the thrust, $\mathbf{M}_O = [L_O, M_O, N_O]^T$ – moments relative to the pole $O$.

Equations (2) are obtained assuming that the missile has two symmetry planes. They are complemented by kinematic relations for rates of roll, pitch and yaw and for components of velocities in relation to the Earth:

$$\dot{\Phi} = P + (R\cos\Phi + Q\sin\Phi)tg\Theta, \tag{3a}$$

$$\dot{\Theta} = Q\cos\Phi - R\sin\Phi, \tag{3b}$$

$$\dot{\Psi} = (R\cos\Phi + Q\sin\Phi)/\cos\Theta, \tag{3c}$$

$$\begin{bmatrix} \dot{x}_g \\ \dot{y}_g \\ \dot{z}_g \end{bmatrix} = \mathbf{L}_{m/g}^{-1} \begin{bmatrix} U \\ V \\ W \end{bmatrix}. \tag{4}$$

## 4. External forces end moments

The external force **F** is the sum of the weight **Q** and the aerodynamic force $\mathbf{F}_{aer}$. Whereas, the aerodynamic moment $\mathbf{M}_O$ relative to the pole $O$ is the sum of the moments generated by the weight $\mathbf{M}_Q$ and the aerodynamic moment $\mathbf{M}_{aer}$:

$$\mathbf{F} = \mathbf{Q} + \mathbf{F}_{aer}, \; \mathbf{M}_O = \mathbf{M}_Q + \mathbf{M}_{aer}. \tag{5}$$

In *Oxyz* system, the weight has following components $\mathbf{Q} = mg[-sT, \;\; cT \cdot sF, \;\; cT \cdot cF]^T$. It produces moment $\mathbf{M}_Q = mg[0, \;\; -x_C \cdot cT \cdot cF, \;\; x_C \cdot cT \cdot sF]^T$.

To calculate aerodynamic forces and moments one has to know the missile velocity relative to air $\mathbf{V}_{aer} = \mathbf{V}_O - \mathbf{V}_w$ where $\mathbf{V}_W$ is the wind (turbulence) velocity.

The aerodynamic forces and moments can be divided into static and dynamic. Static forces and moments are determined on the basis of the nutation angle, which is calculated based on angle of attack $\alpha$ and sideslip angle $\beta$:

$$\alpha = \arctan\frac{W - W_w}{U - U_w}, \; \beta = \arctan\frac{V - V_w}{\sqrt{(U - U_w)^2 + (W - W_w)^2}}, \; \delta = \arcsin\left(\sqrt{\sin^2\beta + \cos^2\beta\sin^2\alpha}\right).$$

While, the dynamic forces and moments are created when the missile is rotating. The resultant aerodynamic force $\mathbf{F}_{aer}$ is equal to the sum of forces set out below:

$$\mathbf{F}_{aer} = \mathbf{F}_D + \mathbf{F}_L + \mathbf{F}_M + \mathbf{F}_{pdf} \text{ or } \mathbf{F}_{aer} = \mathbf{F}_X + \mathbf{F}_N + \mathbf{F}_M + \mathbf{F}_{pdf} . \quad (6)$$

To determine aerodynamic forces and moments acting on the missile the following unit vectors of coordinate systems have to be used: unit vectors ***i***, ***j***, ***k*** of the system *Oxyz* and unit vectors $\boldsymbol{i_a}$, $\boldsymbol{j_a}$, $\boldsymbol{k_a}$ of the aerodynamic system $Ox_ay_az_a$. Summary expressions for these forces and moments are shown in the table below.

| Forces & Moments | General formula | Components in *Oxyz* system | Scalar value | Coefficient & Comments |
|---|---|---|---|---|
| **Aerodynamic forces:** $\mathbf{F}_{aer} = \mathbf{F}_D + \mathbf{F}_L + \mathbf{F}_M + \mathbf{F}_{pdf}$ **or** $\mathbf{F}_{aer} = \mathbf{F}_X + \mathbf{F}_N + \mathbf{F}_M + \mathbf{F}_{pdf}$ | | | | |
| **Static aerodynamic forces** | | | | |
| **Drag force** $\mathbf{F}_D$ | $\mathbf{F}_D = -C_D \frac{\rho V_{aer}^2}{2} S \cdot \boldsymbol{i_a}$ | $\mathbf{F}_D = -C_D \frac{\rho V_{aer}^2}{2} S \cdot \left[\frac{U}{V_{pow}}, \frac{V}{V_{pow}}, \frac{W}{V_{pow}}\right]^T$ | $F_D = C_D \frac{\rho V_{aer}^2}{2} S$ | $C_D = C_{D0} + C_{D\delta 2}\delta^2$<br>$C_D>0$<br>This force is parallel to the trajectory, and is directed opposite to the velocity vector of the missile. |
| **Lift force** $\mathbf{F}_L$ | $\mathbf{F}_L = \frac{\rho V_{aer}^2}{2} S \cdot C_{L\delta} \cdot [\boldsymbol{i_a} \times (\boldsymbol{i} \times \boldsymbol{i_a})]$ | $\mathbf{F}_L = \frac{\rho V_{aer}^2}{2} S \cdot C_{L\delta} \cdot \left[\left(\frac{V^2+W^2}{V_{aer}^2}\right), \left(\frac{-UV}{V_{aer}^2}\right), \left(\frac{-UW}{V_{aer}^2}\right)\right]^T$ | $F_L = C_L \frac{\rho V_{aer}^2}{2} S$ | $C_L = C_{L\delta}\delta = C_{L\delta 0}\delta + C_{L\delta 2}\delta^3$<br>$C_{L\delta} = C_{L\delta 0} + C_{L\delta 2}\delta^2$<br>This force lies in the drag plane and is perpendicular to the trajectory and hence to the velocity of the missile. |
| **Axial force** $\mathbf{F}_X$ | $\mathbf{F}_X = -C_x \frac{\rho V_{aer}^2}{2} S \cdot \boldsymbol{i}$ | $\mathbf{F}_X = -C_x \frac{\rho V_{aer}^2}{2} S [1, \ 0, \ 0]^T$ | $F_X = C_x \frac{\rho V_{aer}^2}{2} S$ | $C_x = C_{x0} + C_{x\delta 2}\delta^2 + C_{x\delta 4}\delta^4$<br>$C_x>0$<br>This force is parallel to the longitudinal axis of the projectile and has opposite sense. |
| **Normal force** $\mathbf{F}_N$ | $\mathbf{F}_N = \frac{\rho V_{aer}^2}{2} S \cdot C_{N\delta} \cdot [\boldsymbol{i} \times (\boldsymbol{i} \times \boldsymbol{i_a})]$ | $\mathbf{F}_N = -\frac{\rho V_{aer}^2}{2} S \cdot C_{N\delta} \cdot \left[0, \frac{V}{V_{aer}}, \frac{W}{V_{aer}}\right]^T$ | $F_N = C_N \frac{\rho V_{aer}^2}{2} S$ | $C_N = C_{N\delta}\delta = C_{N\delta 0}\delta + C_{N\delta 2}\delta^3$<br>$C_{N\delta} = C_{N\delta 0} + C_{N\delta 2}\delta^2$<br>This force is perpendicular to the longitudinal axis of the missile and lies in the drag plane. |
| **Dynamic aerodynamic forces** | | | | |
| **Magnus force** $\mathbf{F}_M$ | $\mathbf{F}_M = \frac{\rho V_{aer}^2}{2} S \left(\frac{Pd}{V_{aer}}\right) C_{N_{p\delta}} \cdot (\boldsymbol{i_a} \times \boldsymbol{i})$ | $\mathbf{F}_M = \frac{\rho V_{aer}^2}{2} S \left(\frac{Pd}{V_{aer}}\right) C_{N_{p\delta}} \cdot \left[0, \frac{W}{V_{aer}}, \frac{-V}{V_{aer}}\right]^T$ | $F_M = \frac{\rho V_{aer}^2}{2} S \left(\frac{Pd}{V_{aer}}\right) C_{N_p}$ | $C_{N_p} = C_{N_{p\delta}}\delta = C_{N_{p\delta 0}}\delta + C_{N_{p\delta 2}}\delta^3$<br>$C_{N_{p\delta}} = C_{N_{p\delta 0}} + C_{N_{p\delta 2}}\delta^2$<br>$C_{N_p} < 0$<br>This force arises when the missile rotates with the angular velocity *P* about the longitudinal *Ox*. It is perpendicular to the drag plane. |
| **Pitch damping force** $\mathbf{F}_{pdf}$ | $\mathbf{F}_{pdf} = \frac{\rho V_{aer}^2}{2} Sd \cdot (C_{Nq} + C_{N\dot{\alpha}}) \left(\frac{d\boldsymbol{i}}{dt}\right)$ | $\mathbf{F}_{pdf} = \frac{\rho V_{aer}^2}{2} S (C_{Nq} + C_{N\dot{\alpha}}) \cdot \left[0, \frac{Rd}{V_{aer}}, \frac{-Qd}{V_{aer}}\right]$ | $F_{pdf} = \frac{\rho V_{aer}^2}{2} S \left(\frac{Q_t d}{V_{aer}}\right) \cdot (C_{Nq} + C_{N\dot{\delta}})$ | $Q_t = \sqrt{Q^2 + R^2}$<br>The angular velocities *Q* and *R* and the rate of change of the nutation angle $\delta$ generate additional dynamic force, which also produce damping moment. |

| Aerodynamic moments $\mathbf{M}_{aer} = \mathbf{M}_{om} + \mathbf{M}_{pdm} + \mathbf{M}_{sdm} + \mathbf{M}_{M}$ | | | | |
|---|---|---|---|---|
| **Static aerodynamic moment** | | | | |
| **Over-turning moment $\mathbf{M}_{om}$** | $\mathbf{M}_{om} = \frac{\rho V_{aer}^2}{2} Sd \cdot C_{M\delta}(\boldsymbol{i}_a \times \boldsymbol{i})$ | $\mathbf{M}_{om} = \frac{\rho V_{aer}^2}{2} Sd \cdot C_{M\delta} \cdot \left[0, \quad \frac{W}{V_{aer}}, \quad \frac{-V}{V_{aer}}\right]^T$ | $M_{om} = \frac{\rho V_{aer}^2}{2} Sd \cdot C_M$ | $C_M = C_{M\delta}\delta = C_{M\delta 0}\delta + C_{M\delta 2}\delta^3$<br>$C_{M\delta} = C_{M\delta 0} + C_{M\delta 2}\delta^2$<br>This moment arises because the centre of pressure does not coincide with the mass centre of missile as well as with the pole $O$. |
| **Dynamic aerodynamic moment** | | | | |
| **Pitch damping moment $\mathbf{M}_{pdm}$** | $\mathbf{M}_{pdm} = \frac{\rho V_{aer}^2}{2} Sd^2 \cdot (C_{Mq} + C_{M\dot{\alpha}})\left(\boldsymbol{i} \times \frac{d\boldsymbol{i}}{dt}\right)$ | $\mathbf{M}_{pdm} = \frac{\rho V_{aer}^2}{2} Sd(C_{Mq} + C_{M\dot{\alpha}}) \cdot \left[0, \quad \frac{Qd}{V_{aer}}, \quad \frac{Rd}{V_{aer}}\right]$ | $M_{pdm} = \frac{\rho V_{aer}^2}{2} Sd\left(\frac{Q_t d}{V_{pow}}\right) \cdot (C_{Mq} + C_{M\dot{\delta}})$ | This moment arises if the missile has angular velocities $Q$ and $R$ and if there is a rate of change of the nutation angle $\delta$. |
| **Spin damping moment $\mathbf{M}_{sdm}$** | $\mathbf{M}_{sdm} = \frac{\rho V_{aer}^2}{2} SdC_{lp} \cdot \left(\frac{Pd}{V_{aer}}\right)\boldsymbol{i}$ | $\mathbf{M}_{sdm} = \frac{\rho V_{aer}^2}{2} SdC_{lp}\left(\frac{Pd}{V_{aer}}\right) \cdot [1, \quad 0, \quad 0]$ | $M_{sdm} = \frac{\rho V_{aer}^2}{2} SdC_{lp}\left(\frac{Pd}{V_{aer}}\right)$ | $C_{lp} < 0$<br>If the missile is rotated about the longitudinal axis, the rotation is decelerated due to air viscosity. |
| **Magnus moment $\mathbf{M}_{pdm}$** | $\mathbf{M}_{M} = \frac{\rho V_{aer}^2}{2} Sd\left(\frac{Pd}{V_{aer}}\right)C \cdot [\boldsymbol{i} \times (\boldsymbol{i}_a \times \boldsymbol{i})]$ | $\mathbf{M}_{M} = \frac{\rho V_{aer}^2}{2} Sd\left(\frac{Pd}{V_{aer}}\right)C_{M_{p\delta}} \cdot \left[0, \quad \frac{V}{V_{aer}}, \quad \frac{W}{V_{aer}}\right]^T$ | $M_{M} = \frac{\rho V_{aer}^2}{2} Sd\left(\frac{Pd}{V_{aer}}\right)C_{M_p}$ | $C_{M_p} = C_{M_{p\delta}}\delta = C_{M_{p\alpha 0}}\delta + C_{M_{p\delta 2}}\delta^3$<br>$C_{M_{p\delta}} = C_{M_{p\delta 0}} + C_{M_{p\delta 2}}\delta^2$<br>This moment arises because the Magnus force is applied outside of the centre of mass. |

*where: $\rho$ – air density, $C_i$ – coefficients of aerodynamic forces and moments, d – diameter of the missile, S – reference area*

Aerodynamic coefficients are determined using PRODAS software [14], which theoretical base can be found in [5]. Exemplary courses are shown in Fig. 2 and 3.

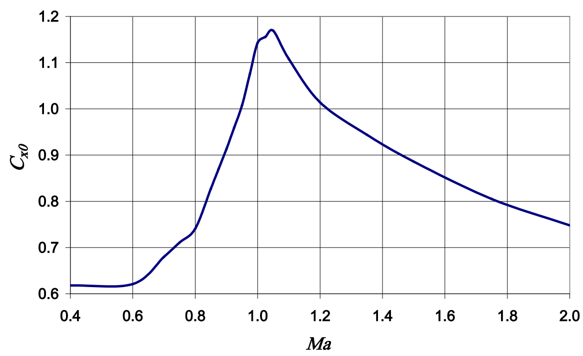


*Fig. 2. Drag coefficient $C_{x0}$*

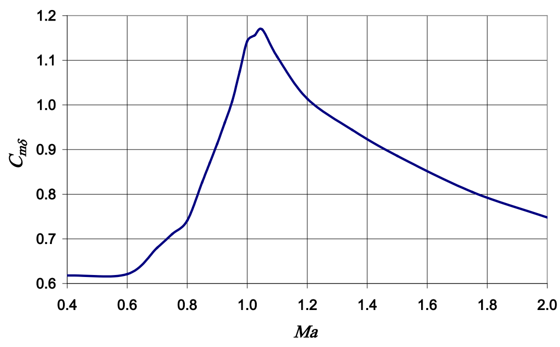


*Fig. 3. Pitch moment coefficient $C_{m\delta}$*

## 5. Model of the turbulence

The wind is dependent on time and space, but very often, it is assumed that it is only function of space $\mathbf{V}_w = \mathbf{V}_w(x_g, y_g, z_g)$. This assumption is based on the Taylor's "frozen turbulence" hypothesis. According to this hypothesis, the advection velocity of the turbulence is much greater than the velocity scale of the turbulence itself. The velocity $\mathbf{V}_w$ has two component – one with the constant value and direction and the second, which is various. In this article, the first component is omitted and the second is treated as the stochastic process representing atmospheric turbulence. To describe this turbulence Shinozuka's method was applied [9, 13, 19, 20]. This method is very useful to numerical simulation of stochastic processes. Originally, it was dedicated to simulate earthquakes. In this method, any stochastic process is written as a sum of periodic functions, amplitudes of which depend on the so-called Power Spectral Density Φ (PSD). Phases of these functions are random "white noise". The formula for *i*-th component of $\mathbf{V}_w$ is as follows:

$$\mathbf{V}_{w\_i}(\mathbf{r}) = \sum_{j=1}^{i}\sum_{l=1}^{L}\left|H_{ij}(\mathbf{\Omega}_l)\right|\sqrt{2\Delta\mathbf{\Omega}}\cos\left(\mathbf{\Omega}_l^{'}\mathbf{r} + \phi_{jl}\right), \tag{7}$$

where: $\mathbf{\Omega}_l$ – the vector of „spatial" frequency, $\mathbf{\Omega}_l^{'}$ – the perturbed vector of „spatial" frequency; $\mathbf{r}=[x_g,y_g,z_g]$ – the vector determining position of the point under consideration; $\phi_{jl}$ – the mutually independent and stochastically variable phase displacements of values 0-2π; **H** – the lower triangular matrix of amplitudes related to the matrix of Power Spectral Density **Φ** by means of the following dependence:

$$\mathbf{\Phi}(\mathbf{\Omega}) = \mathbf{H}(\mathbf{\Omega})\cdot\mathbf{H}^T(\mathbf{\Omega}). \tag{8}$$

Nonzero components of matrix **H**(**Ω**) can be determined if PSD is known:

$$H_{11} = \sqrt{\Phi_{11}}\,,\ H_{21} = \Phi_{21}/H_{11},\ H_{22} = \sqrt{\Phi_{22} - (H_{21})^2}\,,$$

$$H_{31} = \Phi_{31}/H_{11},\ H_{32} = (\Phi_{32} - H_{31}H_{21})/H_{22},\ H_{33} = \sqrt{\Phi_{33} - (H_{31})^2 - (H_{32})^2}\,.$$

As it is above visible, to determine matrix **H** the Power Spectral Density **Φ** must be known. It can be determined on the basis of available measurements of wind field fluctuations, or using specific expressions presented in the literature. One of the most popular is the Dryden's spectrum used in flight mechanics [7, 9, 13]. We can find three variants of spectrums:

- one dimensional spectrum:

$$\mathbf{\Phi}(\Omega_x) = \frac{L_w}{2\pi}\frac{\sigma^2}{\left[1+L_w^2\Omega_x^2\right]^2}\begin{bmatrix} 2\left(1+L_w^2\Omega_x^2\right) & 0 & 0 \\ 0 & 1+3L_w^2\Omega_x^2 & 0 \\ 0 & 0 & 1+3L_w^2\Omega_x^2 \end{bmatrix}, \tag{9a}$$

- two dimensional spectrum:

$$\mathbf{\Phi}(\Omega_x,\Omega_y) = \frac{L_w^2}{4\pi}\frac{\sigma^2}{\left[1+L_w^2\left(\Omega_x^2+\Omega_y^2\right)\right]^{\frac{5}{2}}}\begin{bmatrix} 1+L_w^2\left(\Omega_x^2+4\Omega_y^2\right) & -3\Omega_x\Omega_y L_w^2 & 0 \\ -3\Omega_x\Omega_y L_w^2 & 1+L_w^2\left(4\Omega_x^2+\Omega_y^2\right) & 0 \\ 0 & 0 & 3L_w^2\left(\Omega_x^2+\Omega_y^2\right) \end{bmatrix}, \tag{9b}$$

- three dimensional spectrum:

$$\mathbf{\Phi}(\Omega_x,\Omega_y,\Omega_z) = \frac{2L_w^3}{\pi^2}\frac{\sigma^2}{\left[1+L_w^2\left(\Omega_x^2+\Omega_y^2+\Omega_z\right)\right]^3}\begin{bmatrix} L_w^2\left(\Omega_y^2+\Omega_z^2\right) & -\Omega_x\Omega_y L_w^2 & -\Omega_x\Omega_z L_w^2 \\ -\Omega_y\Omega_x L_w^2 & L_w^2\left(\Omega_x^2+\Omega_z^2\right) & -\Omega_y\Omega_z L_w^2 \\ -\Omega_z\Omega_x L_w^2 & -\Omega_z\Omega_y L_w^2 & L_w^2\left(\Omega_x^2+\Omega_y^2\right) \end{bmatrix}, \tag{9c}$$

where: $L_w$ – the scale of turbulence, $\sigma$ – the standard deviation of turbulence.

On the basis of (7) components of the turbulence in $Ox_gy_gz_g$ system can be calculated as follows:

- for one dimensional spectrum ($y_g$=*const*, $z_g$=*const*):

$$U_{wg}(x_g)=\sum_{l_x=1}^{L_x}\sum_{l_y=1}^{L_y}\left|H_{11}\left(\Omega_{xl_x}\right)\right|\sqrt{2\cdot\Delta\Omega_x}\cos\left[\Omega'_{xl_x}x_g+\phi_{1l_x}\right],\tag{10a}$$

$$V_{wg}(x_g)=\sum_{l_x=1}^{L_x}\sum_{l_y=1}^{L_y}\left|H_{21}\left(\Omega_{xl_x}\right)\right|\sqrt{2\cdot\Delta\Omega_x}\cos\left[\Omega'_{xl_x}x_g+\phi_{1l_x}\right]+\sum_{l_x=1}^{L_x}\sum_{l_y=1}^{L_y}\left|H_{22}\left(\Omega_{xl_x}\right)\right|\sqrt{2\cdot\Delta\Omega_x}\cos\left[\Omega'_{xl_x}x_g+\phi_{2l_x}\right],\tag{10b}$$

$$\begin{aligned}W_{wg}(x_g)=&\sum_{l_x=1}^{L_x}\sum_{l_y=1}^{L_y}\left|H_{31}\left(\Omega_{xl_x}\right)\right|\sqrt{2\cdot\Delta\Omega_x}\cos\left[\Omega'_{xl_x}x_g+\phi_{1l_x}\right]+\sum_{l_x=1}^{L_x}\sum_{l_y=1}^{L_y}\left|H_{32}\left(\Omega_{xl_x}\right)\right|\sqrt{2\cdot\Delta\Omega_x}\cos\left[\Omega'_{xl_x}x_g+\phi_{2l_x}\right]\\&+\sum_{l_x=1}^{L_x}\sum_{l_y=1}^{L_y}\left|H_{33}\left(\Omega_{xl_x}\right)\right|\sqrt{2\cdot\Delta\Omega_x}\cos\left[\Omega'_{xl_x}x_g+\phi_{3l_x}\right],\end{aligned}\tag{10c}$$

– for two dimensional spectrum ($z_g=const$):

$$U_{wg}(x_g,y_g)=\sum_{l_x=1}^{L_x}\sum_{l_y=1}^{L_y}\left|H_{11}\left(\Omega_{xl_x},\Omega_{yl_y}\right)\right|\sqrt{2\cdot\Delta\Omega_x\cdot\Delta\Omega_y}\cos\left[\Omega'_{xl_x}x_g+\Omega'_{yl_y}y_g+\phi_{1l_xl_y}\right],\tag{11a}$$

$$\begin{aligned}V_{wg}(x_g,y_g)=&\sum_{l_x=1}^{L_x}\sum_{l_y=1}^{L_y}\left|H_{21}\left(\Omega_{xl_x},\Omega_{yl_y}\right)\right|\sqrt{2\cdot\Delta\Omega_x\cdot\Delta\Omega_y}\cos\left[\Omega'_{xl_x}x_g+\Omega'_{yl_y}y_g+\phi_{1l_xl_y}\right]\\&+\sum_{l_x=1}^{L_x}\sum_{l_y=1}^{L_y}\left|H_{22}\left(\Omega_{xl_x},\Omega_{yl_y}\right)\right|\sqrt{2\cdot\Delta\Omega_x\cdot\Delta\Omega_y}\cos\left[\Omega'_{xl_x}x_g+\Omega'_{yl_y}y_g+\phi_{2l_xl_y}\right],\end{aligned}\tag{11b}$$

$$\begin{aligned}W_{wg}(x_g,y_g)=&\sum_{l_x=1}^{L_x}\sum_{l_y=1}^{L_y}\left|H_{31}\left(\Omega_{xl_x},\Omega_{yl_y}\right)\right|\sqrt{2\cdot\Delta\Omega_x\cdot\Delta\Omega_y}\cos\left[\Omega'_{xl_x}x_g+\Omega'_{yl_y}y_g+\phi_{1l_xl_y}\right]\\&+\sum_{l_x=1}^{L_x}\sum_{l_y=1}^{L_y}\left|H_{32}\left(\Omega_{xl_x},\Omega_{yl_y}\right)\right|\sqrt{2\cdot\Delta\Omega_x\cdot\Delta\Omega_y}\cos\left[\Omega'_{xl_x}x_g+\Omega'_{yl_y}y_g+\phi_{2l_xl_y}\right]\\&+\sum_{l_x=1}^{L_x}\sum_{l_y=1}^{L_y}\left|H_{33}\left(\Omega_{xl_x},\Omega_{yl_y}\right)\right|\sqrt{2\cdot\Delta\Omega_x\cdot\Delta\Omega_y}\cos\left[\Omega'_{xl_x}x_g+\Omega'_{yl_y}y_g+\phi_{3l_xl_y}\right],\end{aligned}\tag{11c}$$

– for three dimensional spectrum:

$$\begin{aligned}&U_{wg}(x_g,y_g,z_g)=\\&=\sum_{l_x=1}^{L_x}\sum_{l_y=1}^{L_y}\sum_{l_z=1}^{L_z}\left|H_{11}\left(\Omega_{xl_x},\Omega_{yl_y},\Omega_{zl_z}\right)\right|\sqrt{2\cdot\Delta\Omega_x\cdot\Delta\Omega_y\cdot\Delta\Omega_z}\cos\left[\Omega'_{xl_x}x_g+\Omega'_{yl_y}y_g+\Omega'_{zl_z}z_g+\phi_{1l_xl_yl_z}\right],\end{aligned}\tag{12a}$$

$$\begin{aligned}&V_{wg}(x_g,y_g,z_g)=\\&=\sum_{l_x=1}^{L_x}\sum_{l_y=1}^{L_y}\sum_{l_z=1}^{L_z}\left|H_{21}\left(\Omega_{xl_x},\Omega_{yl_y},\Omega_{zl_z}\right)\right|\sqrt{2\cdot\Delta\Omega_x\cdot\Delta\Omega_y\cdot\Delta\Omega_z}\cos\left[\Omega'_{xl_x}x_g+\Omega'_{yl_y}y_g+\Omega'_{zl_z}z_g+\phi_{1l_xl_yl_z}\right]+\\&+\sum_{l_x=1}^{L_x}\sum_{l_y=1}^{L_y}\sum_{l_z=1}^{L_z}\left|H_{22}\left(\Omega_{xl_x},\Omega_{yl_y},\Omega_{zl_z}\right)\right|\sqrt{2\cdot\Delta\Omega_x\cdot\Delta\Omega_y\cdot\Delta\Omega_z}\cos\left[\Omega'_{xl_x}x_g+\Omega'_{yl_y}y_g+\Omega'_{zl_z}z_g+\phi_{2l_xl_yl_z}\right],\end{aligned}\tag{12b}$$

$$\begin{aligned}&W_{wg}(x_g,y_g,z_g)=\\&=\sum_{l_x=1}^{L_x}\sum_{l_y=1}^{L_y}\sum_{l_z=1}^{L_z}\left|H_{31}\left(\Omega_{xl_x},\Omega_{yl_y},\Omega_{zl_z}\right)\right|\sqrt{2\cdot\Delta\Omega_x\cdot\Delta\Omega_y\cdot\Delta\Omega_z}\cos\left[\Omega'_{xl_x}x_g+\Omega'_{yl_y}y_g+\Omega'_{zl_z}z_g+\phi_{1l_xl_yl_z}\right]+\\&+\sum_{l_x=1}^{L_x}\sum_{l_y=1}^{L_y}\sum_{l_z=1}^{L_z}\left|H_{32}\left(\Omega_{xl_x},\Omega_{yl_y},\Omega_{zl_z}\right)\right|\sqrt{2\cdot\Delta\Omega_x\cdot\Delta\Omega_y\cdot\Delta\Omega_z}\cos\left[\Omega'_{xl_x}x_g+\Omega'_{yl_y}y_g+\Omega'_{zl_z}z_g+\phi_{2l_xl_yl_z}\right]+\\&+\sum_{l_x=1}^{L_x}\sum_{l_y=1}^{L_y}\sum_{l_z=1}^{L_z}\left|H_{33}\left(\Omega_{xl_x},\Omega_{yl_y},\Omega_{zl_z}\right)\right|\sqrt{2\cdot\Delta\Omega_x\cdot\Delta\Omega_y\cdot\Delta\Omega_z}\cos\left[\Omega'_{xl_x}x_g+\Omega'_{yl_y}y_g+\Omega'_{zl_z}z_g+\phi_{3l_xl_yl_z}\right].\end{aligned}\tag{12c}$$

Additional subscript "g" shows that velocity components are determined in $Ox_g y_g z_g$ coordinate system.

For calculations, boundary values of „spatial" frequency must be defined:

$$\Omega_{x\,\mathrm{lower}} \le \Omega_x \le \Omega_{x\,\mathrm{upper}}\,,\ \Omega_{y\,\mathrm{lower}} \le \Omega_y \le \Omega_{y\,\mathrm{upper}}\,,\ \Omega_{z\,\mathrm{lower}} \le \Omega_z \le \Omega_{z\,\mathrm{upper}}\,, \tag{13}$$

and next ranges of frequencies are respectively divided into $L_x$, $L_y$ and $L_z$ subintervals in the manner:

$$\Delta\Omega_x = (\Omega_{x\,\mathrm{upper}} - \Omega_{x\,\mathrm{lower}})/L_x\,,\ \Delta\Omega_y = (\Omega_{y\,\mathrm{upper}} - \Omega_{y\,\mathrm{lower}})/L_x\,,\ \Delta\Omega_z = (\Omega_{z\,\mathrm{upper}} - \Omega_{z\,\mathrm{lower}})/L_x\,. \tag{14}$$

The subsequent values of frequencies in (10) are calculated with formulas:

$$\Omega_{xl_x} = \Omega_{x\,\mathrm{lower}} + (l_x - 1)\Delta\Omega_x\,,\ \Omega_{yl_y} = \Omega_{y\,\mathrm{lower}} + (l_y - 1)\Delta\Omega_y\,,\ \Omega_{zl_z} = \Omega_{z\,\mathrm{lower}} + (l_z - 1)\Delta\Omega_z\,. \tag{15}$$

The perturbed vector of „spatial" frequency $\mathbf{\Omega}_l^{'}$ in (7) is randomly perturbed vector $\mathbf{\Omega}_l$, which is determined to avoid periodicity of the simulated turbulence. It has following components:

$$\Omega_{xl_x}^{'} = \Omega_{xl_x} + \delta\Omega_{xl_x}\,,\ \Omega_{yl_y}^{'} = \Omega_{yl_y} + \delta\Omega_{yl_y}\,,\ \Omega_{zl_z}^{'} = \Omega_{zl_z} + \delta\Omega_{zl_z}. \tag{16}$$

Each perturbation must satisfy the condition which e.g. for $x$ component has the form:

$$\left|\delta\Omega_{xl_x}\right| << 0.5\cdot\Delta\Omega_x\,,\ \left|\delta\Omega_{yl_y}\right| << 0.5\cdot\Delta\Omega_y\,,\ \left|\delta\Omega_{zl_z}\right| << 0.5\cdot\Delta\Omega_z\,. \tag{17}$$

Phase displacements $\phi_{jl_x}$, $\phi_{jl_x l_y}$, $\phi_{jl_x l_y l_z}$, ($j = 1, 2, 3$) are mutually independent, randomly variable, and included in the range of 0-2π.

## 6. Results of simulations

Simulations were performed for the missile ICP-1 which is used by Polish Military Forces as a target for antiaircraft training reason (Fig. 4). The basic data of the missile are as follows: initial mas 5.36 kg, fuel mass 1.13 kg, diameter 57 mm, length 1100 mm, engine-working time 0.7 sec.

At the beginning of simulations, the described above model of missile motion was tested by comparing its results with data recorder during real firing tests. In Fig. 5 and 6, we can see comparison for flight velocity and trajectory for the initial conditions: the pitch angle $\Theta=45^0$, the initial velocity $V_{aer}$=40 m/s. We can see good comparison between theoretical calculations and real data despite of differences between theoretically calculated and measured thrust – Fig. 7.

*Fig. 4. ICP-1 missile*

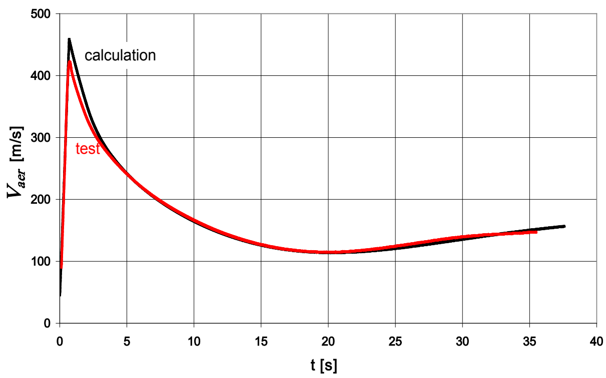


*Fig. 5. Flight velocity of the missile*

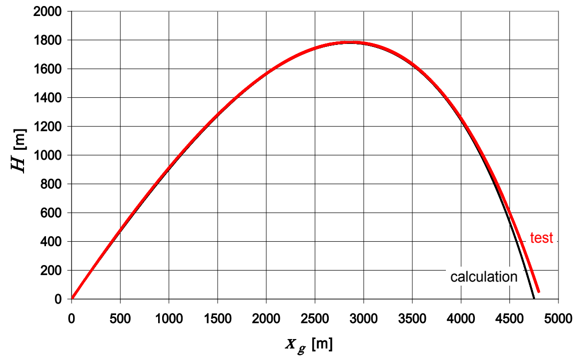


*Fig. 6. Trajectory of the missile*

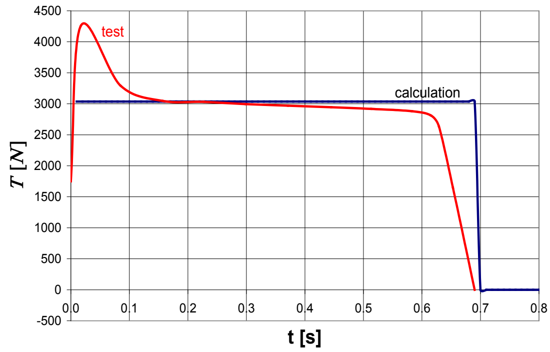


*Fig. 7. Theoretical and measured thrust*

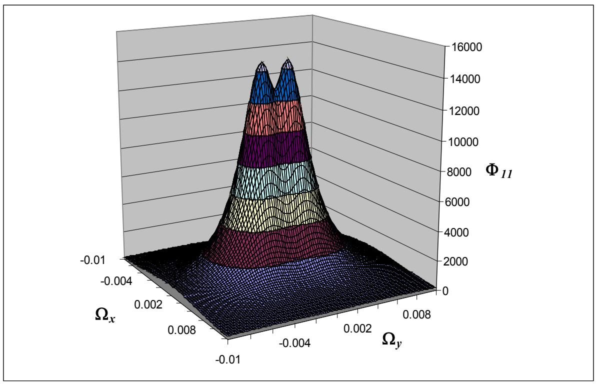


*Fig. 8. PSD $\Phi_{11}$ component*

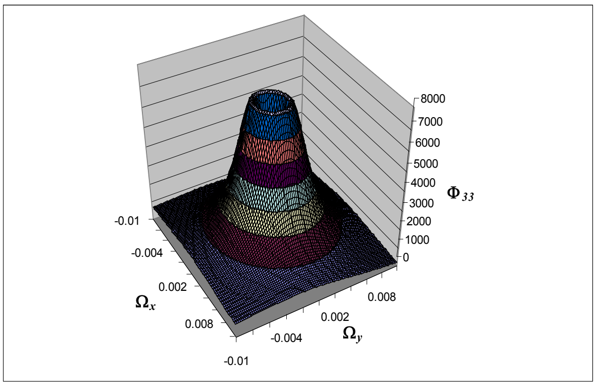


*Fig. 9. PSD $\Phi_{33}$ component*

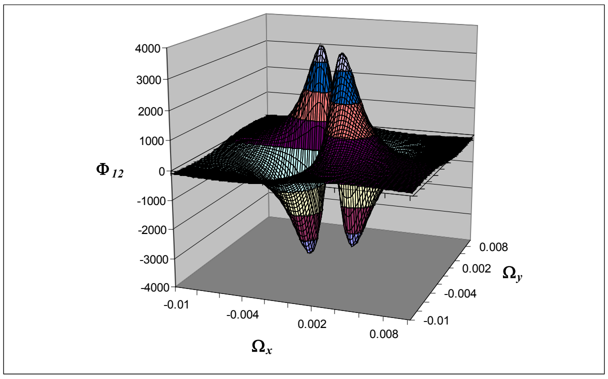


*Fig. 10. PSD $\Phi_{12}$ component*

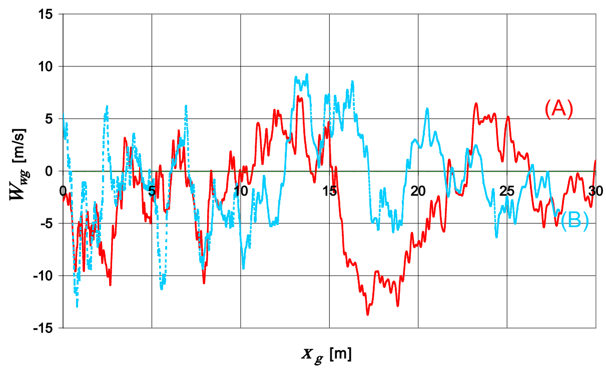


*Fig. 11. $W_{wg}$ component of turbulence*

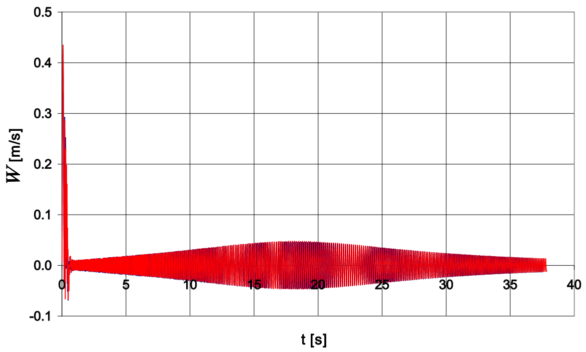


*Fig. 12. W component of linear velocity*

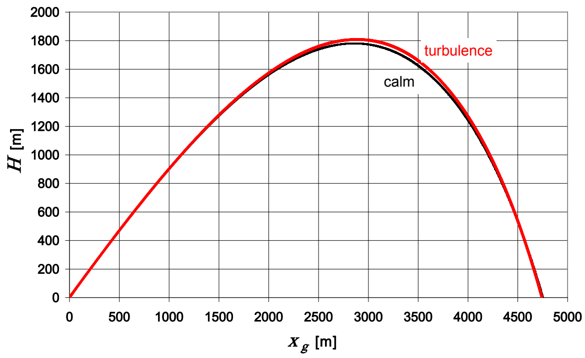


*Fig. 13. Vertical trajectory*

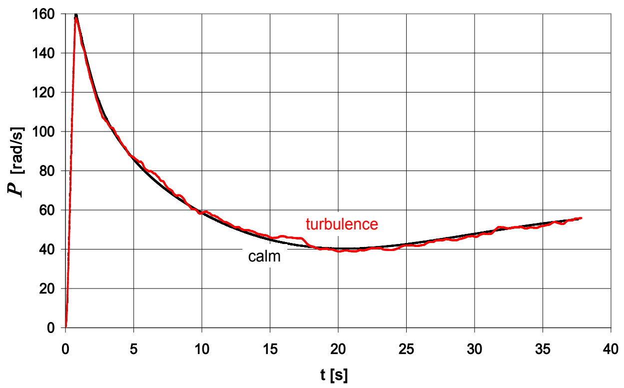


*Fig. 14. Rolling angular velocity P*

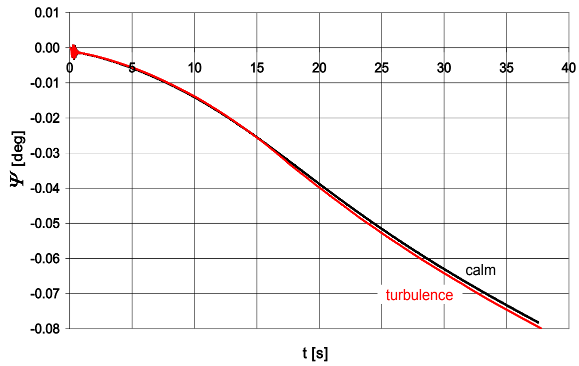


*Fig. 15. Yaw angle Ψ*

Next simulations were performed including shown above stochastic description of the turbulence. The two dimensional PSD were used. Components of the PSD are presented in Fig. 8-10. Parameters of turbulence were as follows: the scale of turbulence $L_w$ =400 m, the standard deviation of turbulence $\sigma$ =5 m/s. During each simulation, different profile of turbulence was obtained. It is shown in Fig. 11 where exemplary courses of $W_{wg\,t}(t)$ turbulence component for two simulations are presented. As it was assumed, we can see that the courses are different each other although they both have the same parameters of stochastic description.

Figure 12-15 show courses of a few flight parameters for calm and turbulent atmosphere versus time. They were obtained for the same initial conditions as above i.e. $\Theta$=45$^0$, $V_{aer}$=40 m/s. For the sake of comparison, each diagram also shows results for the case of calm atmosphere. They are represented with a black dotted line. We can find only small influence of turbulence on some courses. The most visible effect is for the rolling angular velocity $P$ (Fig. 14) and for the yaw angle $\Psi$ (Fig. 15). However, detailed analysis shows that even small disturbances of the flight parameters cause important influence on the point of missile fall. Fig. 16 presents these points obtained for twenty-four simulations for the pitch angle equal to 40$^0$. The coordinates of the fall point without turbulence are respectively $x_g$=4407.6 m and $y_g$=-1.752 m. It means that the trajectory of the missile deviates to the left. In the case of turbulence, the average values of coordinates are as follows: $x_{g\,av}$=4362.75m and $y_{g\,av}$=-1.74 m. Their standard deviations are equal to: $\sigma_x$=58.47 m and $\sigma_y$ =0.015 m. It shows that turbulence strongly impacts on the firing range of missile. It is important if the high precision is required. Comparing shown above $x_g$ coordinates we can see that the turbulence reduces the range of the missile. The reason is that the mean aerodynamic-drag coefficient increases because of the increased nutation angle (Fig. 16).

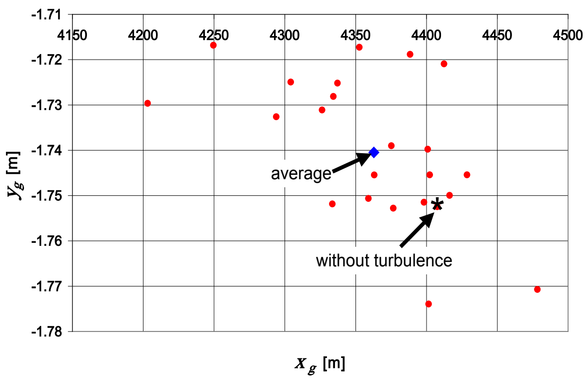


*Fig. 16. Points of the missile fall on the horizontal plane $Ox_gy_g$*

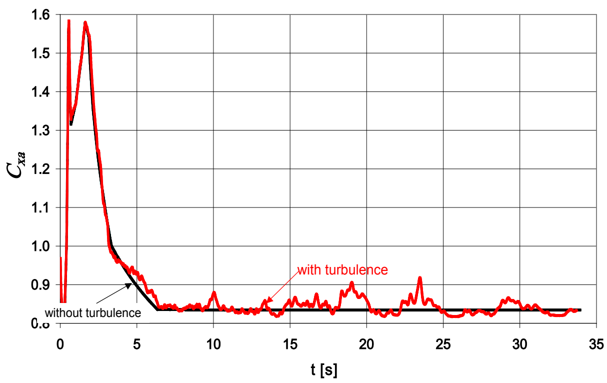


*Fig. 17. Aerodynamic drag coefficient during missile flight*

## 7. Conclusions

The conducted analysis has proved that the effect of turbulence on the missile accuracy may be essential and should be taken into account when planning the precise firing. Stochastic nature of the atmospheric turbulence results in the random distribution of points of fall. Turbulences increase the nutation angle during the missile flight and result in the reduction of the range of firing. Further studies will cover the question of determining final parameters of the missile flight in the wind, depending on initial pitch angle and parameters that describe the wind field.

## References

[1] Baranowski, L., *Effect of The Mathematical Model and Integration Step on The Accuracy of The Results of Computation of Artillery Projectile Flight Parameters*, Bulletin of the Polish Academy of Sciences – Technical Sciences, No. 61 (2), pp. 475-484, 2013.
[2] Carlucci, D. E., Jacobson, S. S., Ballistics – *Theory and Design of Guns and Ammunition*, CRC Press, 2007.
[3] Davis, L., Follin, J. W., Blitzer, L., *Exterior Ballistics of Rockets*, D. Van Nostrad Company Inc., 1958.
[4] Dmitriewskij, A. A., *External Ballistics*, Mashinostroenie, 1979.
[5] Engineering Design Handbook – *Design for Control of Projectile Flight Characteristics*, Headquaters U.S. Army Materiel Command, September 1996.
[6] Gacek, J., *Exterior Ballistics – Part I and II*, Military University of Technology, 1998.
[7] Holbit, F. M., *Gust Loads on Aircraft: Concepts and Applications*, AIAA Education Series, Washington D.C. 1998
[8] Kowaleczko, G., *Evaluation of Jet Damping Effect on Flight Dynamics of a Homing Guided Missile*, Journal of Theoretical and Applied Mechanics, Vol. 54, No. 3, 2016.
[9] Kowaleczko, G., Żyluk, A., *Influence of Atmospheric Turbulence on Bomb Release*, Journal of Theoretical and Applied Mechanics, Vol. 47, No. 1, 2009.
[10] Kurow, W. D., Dolzanskij, J. M, *Basics of Designing of Propellant Rockets*, State Scientific and Technical Publishing Inc. Oborongiz, 1961.
[11] Mattingly, J. D., *Elements of Propulsion, Gas Turbines and Rockets*, AIAA Ed. Series, 2006.
[12] McCoy, R.L., *Modern Exterior Ballistics*, Schifler Publishing Ltd., 2012.
[13] Mnitowski, S., *Modeling of Aircraft Flight in Turbulent Atmosphere*, doctoral thesis, Military University of Technology, 2006.
[14] *PRODAS Software v.3*, Arrow Tech Associates Inc., 2008.
[15] Quarelli, M. B., Cameron, J., Balaram, B., Baranwal, M., Bruno, A., *Modeling and Simulation of Flight Dynamics of Variable Mass System*, Space Conference and Exposition, San Diego, AIAA 2014-4454, 2014.
[16] Rosser, J., Newton, R., Gross, G., *Mathematical Theory of Rocket Flight*, McGraw Hill Book Company Inc., 1947.
[17] Shapiro, J., *Exterior Ballistics*, published by Ministry of Defence, 1956.
[18] Shinozuka, M., *Simulation of Multivariate and Multidimensional Random Processes*, Journal of the Acoustical Society of America, Vol. 49, 1971.
[19] Shinozuka, M., Jan, C.-M., *Digital Simulations of Random Processes and Its Applications*, *Journal of Sound and Vibrations*, No. 25, 1972.
[20] Thomson, W. T., *Equations of Motion for the Variable Mass System,* AIAA Journal, Vol. 4. No. 4, 766-768, 1965.
[21] Thomson, W. T., *Jet Damping of Solid Rocket: Theory and Flight Results*, AIAA Journal, Vol. 3, No. 3, pp. 413-417, 1965.
[22] Thomson, W. T., *Introduction to Space Dynamics*, Dover Publications Inc., 1986.

[23] Torecki, S., *Rocket Propulsion*, Wydawnictwa Komunikacji i Łączności, 1984.
[24] Turner, M., *Rocket and Spacecraft Propulsion – Principles, Practice and New Developments*, Springer Verlag, 2009.